CeO_2 Nanorods and Gold Nanocrystals Supported on CeO_2 Nanorods as Catalyst

P. X. Huang,[†] F. Wu,[†,‡] B. L. Zhu,[§] X. P. Gao,*[,†] H. Y. Zhu,*[,||] T. Y. Yan,[†] W. P. Huang,[§] S. H. Wu,[§] and D. Y. Song[†]

Institute of New Energy Material Chemistry, Department of Materials Chemistry, Nankai University, Tianjin 300071, China, School of Chemical Engineering and Environmental, Beijing Institute of Technology, Beijing 100081, China, Department of Chemistry, Nankai University, Tianjin 300071, China, and Inorganic Materials Research Program, School of Physical and Chemical Sciences, Queensland University of Technology, GPO Box 2434, Brisbane, Qld 4001, Australia

Received: June 4, 2005; In Final Form: August 23, 2005

The formation mechanism of uniform CeO_2 structure at the nanometer scale via a wet-chemical reaction is of great interest in fundamental study as well as a variety of applications. In this work, large-scale well-crystallized CeO_2 nanorods with uniform diameters in the range of 20−30 nm and lengths up to tens of micrometers are first synthesized through a hydrothermal synthetic route in 5 M KOH solution at 180 °C for 45 h without any templates and surfactants. The nanorod formation involves dehydration of CeO_2 nanoparticles and orientation growth along the $\langle 110 \rangle$ direction in KOH solution. Subsequently, gold nanoparticles with crystallite sizes between 10 and 20 nm are loaded on the surface of CeO_2 nanorods using $HAuCl_4$ solution as the gold source and $NaBH_4$ solution as a reducing agent. The synthesized Au/CeO_2 nanorods demonstrate a higher catalytic activity in CO oxidation than the pure CeO_2 nanorods.

I. Introduction

As an important class of nanomaterials, the nanorod has attracted enormous technological and scientific interest.[1] In synthesizing metal oxide nanorods, such as ZnO,[2,3] Al_2O_3,[4,5] MgO,[6] CuO,[7,8] SnO_2,[9] MnO_2,[10] Co_3O_4,[11] V_2O_5,[12] and Eu_2O_3,[13] many approaches have been applied in the past several years, including thermal evaporation, microemulsion method, hydrothermal synthesis, template methods, and electrochemical deposition technique. Hydrothermal reaction under moderate conditions is an effective approach in synthesizing nanosize crystals of inorganic oxides and hydroxides. In many cases, alkaline solution is used in the hydrothermal synthesis in which the shape and size of the crystals are well-controlled. For example, anatase and titanate nanotubes and nanorods were obtained hydrothermally in NaOH solution,[14−17] and lanthanide hydroxide nanowires were synthesized successfully via hydrothermal reaction in KOH solution.[18] The hydroxide nanorods or titanate nanorods can be converted into the corresponding oxide nanorods through a subsequent dehydration process at high temperature.

Ultrafine CeO_2 particles of regular shape and uniform size are desired in a variety of applications, i.e., ceramic ingredient, fluorescent powder, polishing agent, catalyst carrier, catalyst for the exhaust gas treatment from automobiles, and solid electrolyte for solid oxide fuel cells.[19−22] Recently, it has been reported that the polycrystalline CeO_2 nanowires can be fabricated in anodic alumina membranes (AAM) as templates,[23,24] and crystalline CeO_2 nanorods can be formed through a surfactant assemblage because the surfactant in water can form a chain structure.[25−27] The formation mechanism of the uniform CeO_2 nanorod, via a wet chemical reaction, is of great interest in fundamental study. Also, it has been reported that CeO_2 and rare earth oxide nanocrystals can significantly increase the catalytic activity of dispersed Au nanoparticles for CO oxidation.[28−32] The decoration of Au nanoparticles on the support of stable CeO_2 nanorods could efficiently prevent Au nanoparticles from the agglomeration. In the present study, we report a simple approach for the synthesis of large-scale CeO_2 nanorods with single crystalline structure in alkaline solution, without any templates and surfactants. Subsequently, gold nanoparticles are loaded on the so-fabricated CeO_2 nanorods by using $HAuCl_4$ solution as a gold source and $NaBH_4$ solution as a reducing agent. The catalytic activity of Au/CeO_2 nanorods in CO oxidation is measured.

II. Experimental Section

1. Sample Preparation and Characterization. In a typical synthesis, metallic cerium was first dissolved in concentrated hydrochloride acid to obtain cerium chloride solution, and 5 M KOH solution was added gradually into the cerium chloride solution under stirring until the cerium ions precipitate completely. The precipitates ($CeO_2 \cdot nH_2O$) were aged for 30 min in air and then washed repeatedly with deionized water to remove Cl^- anions in the precipitates. The wet precipitates were then mixed with 5 M KOH solution (40 mL) using an ultrasonic bath. The obtained mixture was transferred in a stainless autoclave with a poly(tetrafluoroethylene) (PTFE) container and maintained at 180 °C for different reaction durations. The solid was recovered from the autoclaved mixture, rinsed with water until a value of about pH 7 was reached. Gold nanoparticles were loaded on the CeO_2 nanorods by dispersing 0.1 g of the nanorods in 40 mL of 0.1 M $HAuCl_4$ solution. The impregnated nanorods were separated by centrifugation, and $NaBH_4$ solution (10 mL, 0.1 M) was added to the solid. The solid was then recovered, rinsed with deionized water to remove Cl^- anions, and dried at 100 °C. The so-obtained product (CeO_2 nanorods) was further dried at 60 °C in air for 1 day. The microstructure of the prepared CeO_2 powders was characterized by transmission

* To whom correspondence should be addressed. E-mail: xpgao@nankai.edu.cn (X.P.G.); hy.zhu@qut.edu.au (H.Y.Z.).
[†] Department of Materials Chemistry, Nankai University.
[‡] Beijing Institute of Technology.
[§] Department of Chemistry, Nankai University.
[||] Queensland University of Technology.

10.1021/jp052978u CCC: \$30.25
Published on Web 09/23/2005

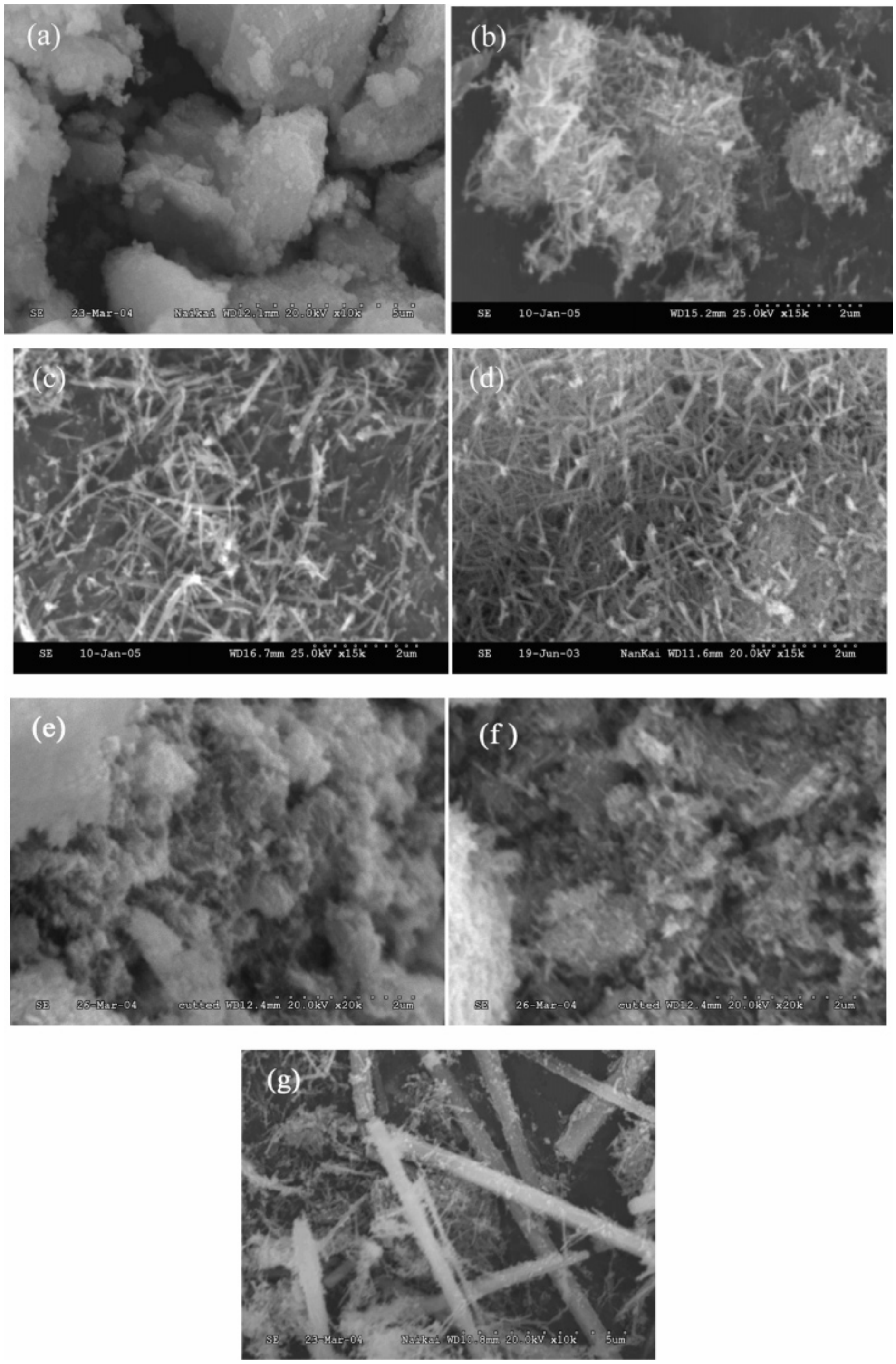

Figure 1. SEM images of CeO_2 nanorods synthesized at different reaction conditions: (a) before the hydrothermal treatment, (b) 5 M KOH at 180 °C for 4 h, (c) 5 M KOH at 180 °C for 24 h, (d) 5 M KOH at 180 °C for 45 h, (e) 5 M KOH at 150 °C for 45 h, (f) 10 M KOH at 150 °C for 45 h, and (g) 10 M KOH at 180 °C for 45 h.

electron microscopy (TEM; FEI Tecnai 20) and X-ray diffraction (XRD, Rigaku D/max-2500) with a Cu Kα radiation. Since the as-synthesized nanoparticles were suspended in solution, a droplet of it was also deposited on a Cu grid covered with a carbon film for TEM analysis. X-ray photoelectron spectra (XPS) analyses were investigated using PHI-5300 ESCA in order to assess the chemical state and element distribution on the catalyst surface.

2. Catalytic Activity. The catalytic activity measurements of the catalysts for CO oxidation were carried out in a fixed bed flow microreactor (7 mm i.d.) under atmospheric pressure using 50 mg of catalyst powder doped with 2 g of fine quartz sand. The reaction gas mixture consisting of 1% CO balanced with air is passed through the catalyst bed at a total flow rate of 33.6 mL/min. The reactant and product composition were analyzed on-line by a GC-508A gas chromatograph equipped with a thermal conductivity detector (TCD).

III. Results and Discussion

Scanning electron microscopy (SEM) images of CeO_2 nanorods synthesized at different hydrothermal reaction conditions are shown in Figure 1. The big agglomerated particles are obtained before the hydrothermal treatment. It can be seen that

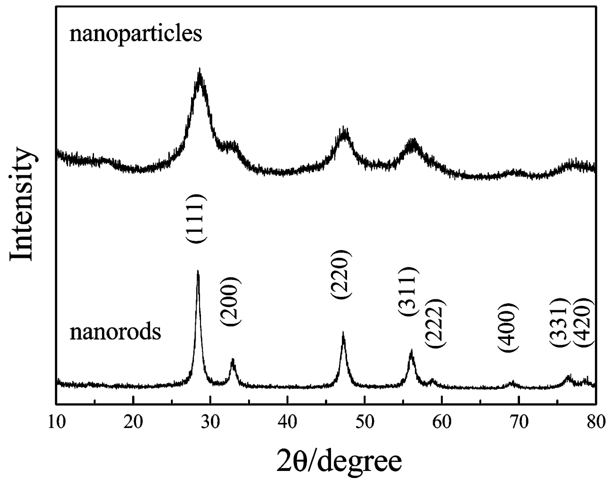

Figure 2. XRD patterns of the CeO_2 nanorods synthesized at 180 °C for 45 h and $CeO_2 \cdot nH_2O$ nanoparticles.

CeO_2 nanorods can be formed at the hydrothermal temperature of 180 °C for 4 h though some nanoparticles still coexisted. Longer reaction duration of the hydrothermal treatment improves of the purity of CeO_2 nanorods and enhances the aspect ratio of CeO_2 nanorods. The alkaline concentration and hydrothermal temperature are observed to have a strong effect on the structure and morphological features of the resulting CeO_2 nanorods. The morphological transformation from particles to nanorods is not complete when the hydrothermal temperature is below 150 °C at 5 or 10 M KOH solution, as shown in Figure 1e,f. It reveals that the hydrothermal temperature is a key parameter that influences the nucleation and crystal growth of CeO_2 nanorods, which is also found for the preparation of titanate nanorods under the hydrothermal condition in NaOH solution.[17] However, the shape of the hydrothermal products is irregular when the alkaline concentration is higher than 5 M at 180 °C. In particular, the large quantity of thicker rods attached with thin nanorods is formed in 10 M KOH solution at 180 °C, indicating that some nanorods further grow and become thicker and longer at the expense of thinner nanorods being dissolved in the higher alkaline concentration.

The XRD patterns of CeO_2 nanorods synthesized at 180 °C for 45 h and $CeO_2 \cdot nH_2O$ nanoparticles are illustrated in Figure 2. All the diffraction peaks for the products before and after hydrothermal treatment in alkaline solution can be indexed to (111), (200), (220), (311), (222), (400), (331), and (420) phases, corresponding to a face-centered cubic (*fcc*) fluorite structure for CeO_2 (JCPDS Card No. 43-1002). There are not any other impurities of the hexagonal structure of $Ce(OH)_3$ or $Ce(OH)CO_3$ detected. It is well-known that the Ce(III) oxidation state is unstable as compared with the Ce(IV) oxidation state in alkaline solution and in the presence of air. From the Ce3d core level peak in the XPS spectra shown in Figure 3, it is clear that the cerium exists as the Ce(IV) oxidation state (882.8 eV), without any impurity of the Ce(III) oxidation state. Also, the XPS peak centered at 529.6 eV corresponds to the O^{2-} contribution.[33] Thus, the XPS-detected binding energies of Ce3d and O1s are in agreement with the standard CeO_2. Thermal gravimetrical analysis (TGA) of $CeO_2 \cdot nH_2O$ nanoparticles indicates a mass loss of about 10.7 wt % below 600 °C, due to the loss of water from the sample. Both nanoparticles and nanorods exhibit a light yellow color, similar to the standard CeO_2. Therefore, the nanoparticles are deduced to be

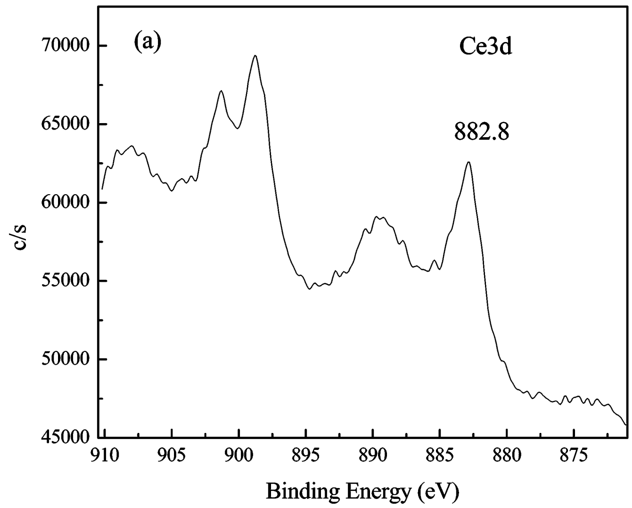

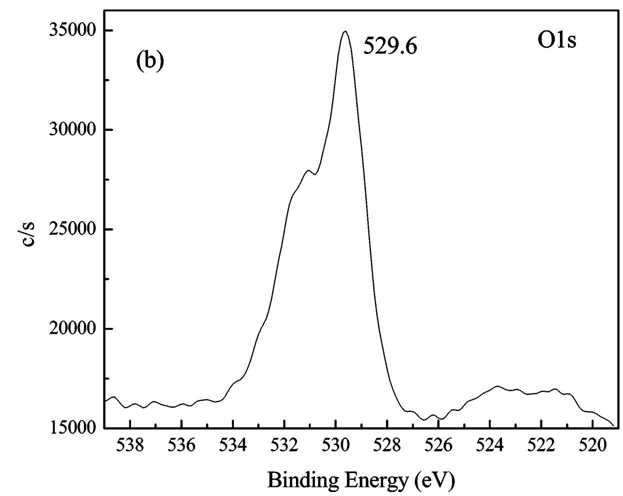

Figure 3. Ce3d (a) and O1s (b) core level spectra observed for CeO_2 nanorods synthesized at 180 °C for 45 h.

$CeO_2 \cdot 1.1H_2O$, and the synthesis process of CeO_2 nanorods can be described as follows:

$$4Ce^{3+} + 12OH^- + O_2 + (4n - 6)H_2O \rightarrow 4(CeO_2 \cdot nH_2O)$$

$$CeO_2 \cdot nH_2O \rightarrow CeO_2 + nH_2O$$

The XRD peaks for $CeO_2 \cdot 1.1H_2O$ nanoparticles are obviously broader, compared with those of the nanorods, indicating that the crystallites of the nanoparticles are smaller than those in the CeO_2 nanorods. The hydrothermal treatment in alkaline solution at 180 °C results in a remarkable improvement in crystallinity. As can be seen clearly from TEM images of the nanorods synthesized at 180 °C for 45 h and nanoparticles (Figure 4), we obtained the straight CeO_2 nanorods of a high purity with uniform diameters in the range of 20−30 nm and lengths up to tens of micrometers (Figure 4a). It is also confirmed by energy-dispersive X-ray spectra (EDS, Figure 4b) that there are not any impurities, indicating that sodium ions and chlorides are completely removed during washing. Cu and C signals are coming from the Cu grid and carbon film supporting the specimen in TEM observation. The selected area electron diffraction (SAED) pattern (insert in Figure 4c) indicates the single crystalline nature of the CeO_2 nanorods with a face-centered cubic structure, and this is consistent with the XRD results. The calculated interference fringe spacing in the HRTEM image is about 0.31 nm, which is consistent with the

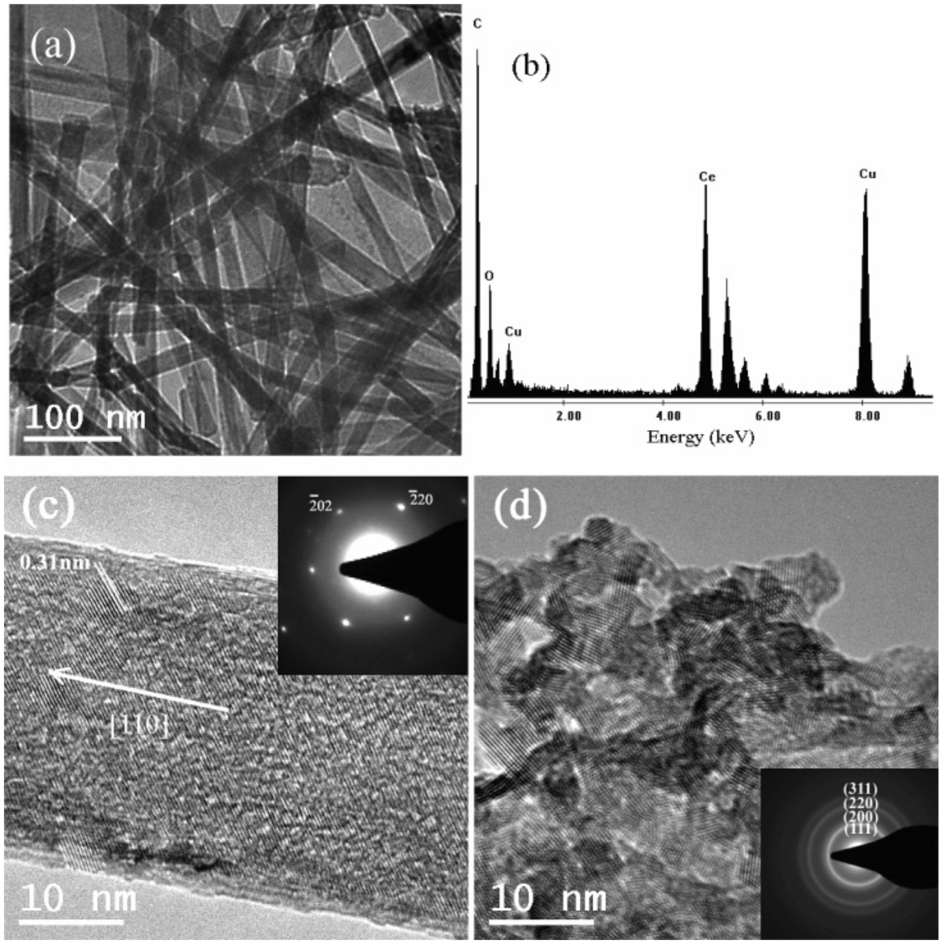

Figure 4. TEM images (a) and EDS (b) of the CeO_2 nanorods synthesized at 180 °C for 45 h. The HRTEM images of the CeO_2 nanorods and $CeO_2{\cdot}nH_2O$ nanoparticles are shown in c and d. The inserts in c and d are SAED of individual CeO_2 nanorod and $CeO_2{\cdot}nH_2O$ nanoparticles, respectively.

interplanar distance of the (111) plane in the cubic fluorite structure. This suggests that the preferred orientation growth of the individual CeO_2 nanorod is along the ⟨110⟩ direction,[34] similar to that of the CeO_2 nanorods obtained by PEG surfactant-assisted preparation.[26] The HRTEM image and SAED pattern also confirm that the precursor nanoparticles have a polycrystalline structure with smaller crystallite sizes of 6−9 nm (Figure 4d). Therefore, the hydrothermal treatment in alkaline solution is essential to the formation of large-scale CeO_2 nanorods via the orientation growth.

The nanorods of titanate,[16,17] lanthanide hydroxide,[18] and CuO[8] have been synthesized hydrothermally in a concentrated alkaline solution without any templates and surfactants. It appears that there are common features and a probably common mechanism for the formation of these metal oxides and hydrous oxides. We believe that the Ostwald ripening process, in which larger crystallites grow at the expense of smaller crystallites being dissolved,[35] is involved in the structure transformation from the polycrystalline $CeO_2{\cdot}1.1H_2O$ nanoparticles to the single crystalline CeO_2 nanorods during the hydrothermal treatment at 180 °C for 45 h. The above formation mechanism is different from the polycrystalline or nanocrystalline CeO_2 nanowires prepared by the AAM method.[24,25] Also the OH^- concentration in the reaction system could be the key factor controlling the growth rate of different crystal faces and leading to the formation of a rodlike morphology. In the hydrothermal process, the nanosize CeO_2 crystallinates grow along the ⟨110⟩ direction in the concentrated KOH solution by consuming the $CeO_2{\cdot}1.1H_2O$ precipitates, yielding the rodlike structure.

As shown in Figure 5a, the gold nanoparticles are dispersed effectively on the surface of the CeO_2 nanorods synthesized at 180 °C for 45 h and are not agglomerated. The gold nanoparticles on the CeO_2 nanorods have crystallite sizes between 10 and 20 nm. The interplanar spacing of the gold nanoparticle in HRTEM images (Figure 5b) is ca. 0.24 nm, corresponding to the interplanar distance of the (111) plane of *fcc* Au nanocrystal as found in Au/TiO_2 nanotubes.[36,37] The energy-dispersive X-ray spectrum (EDS, as inserted in Figure 5a) confirms the presence of Au element. The observation of the diffractions peaks of metallic gold (JCPDS Card No. 04-0784) in the XRD pattern (Figure 6) confirms that gold exists as metallic particles. It is noted that the surface of the CeO_2 nanorods, after the decoration of gold nanoparticles, is roughened as compared to that of the pure CeO_2 nanorods, indicating a strong interaction at the interface of Au nanoparticles and CeO_2 nanorods during the reduction in $HAuCl_4$ and $NaBH_4$ solution. Moreover, the surface of a gold nanoparticle is covered by a thin discrete layer of the cerium oxides (1−2 nm) attributed to migration of the oxide onto the gold surface.[38] The interference fringe of the (111) plane of inner CeO_2 nanorods is clearly observed in the HRTEM image (Figure 5b), demonstrating a good crystallinity and a high stability of CeO_2 nanorods after the decoration of Au nanoparticles. Similarly, gold nanoparticles supported on CeO_2 nanoparticles are also found with the preferential (111) plane of *fcc* Au nanocrystal (interplanar spacing is ca. 0.24 nm as shown in Figure 5d). However, the dispersed state of gold nanoparticles on CeO_2 nanoparticles is relatively poor as compared with that on CeO_2 nanorods.

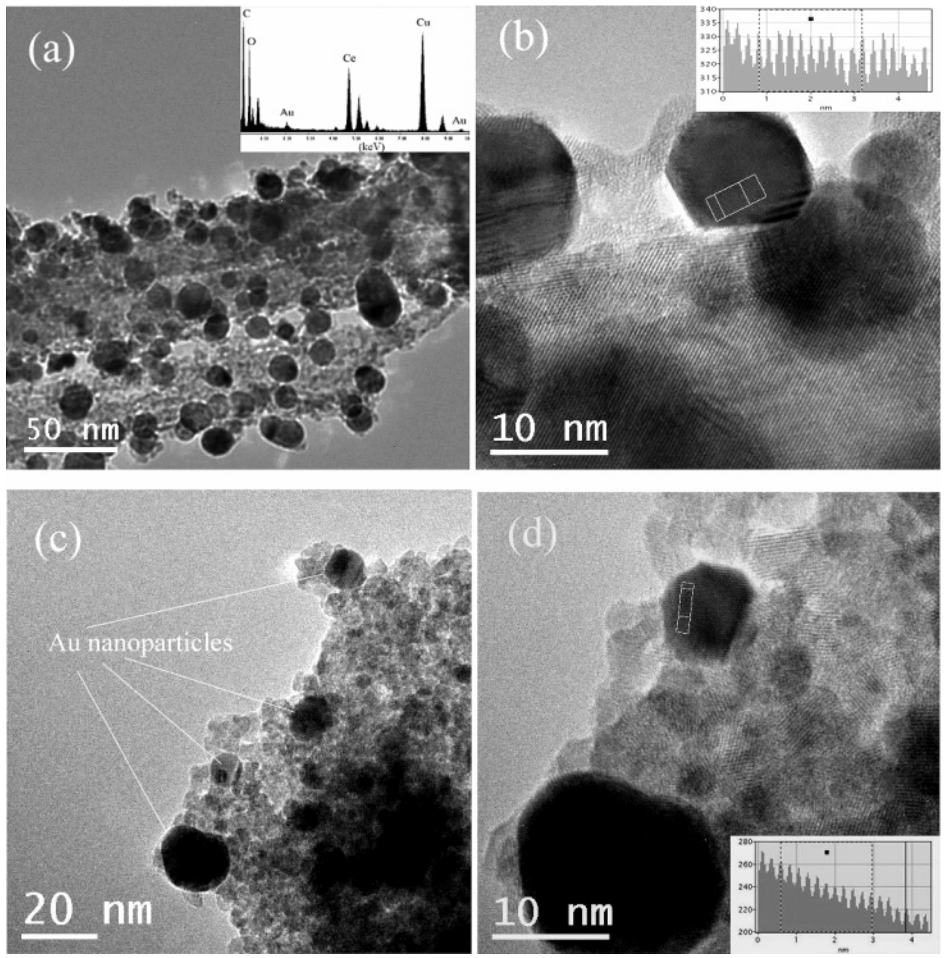

Figure 5. TEM and HRTEM images of Au/CeO$_2$ nanorods (a and b) and Au/CeO$_2$ nanoparticles (c and d). The EDS spectrum of Au/CeO$_2$ nanorods is inserted in a.

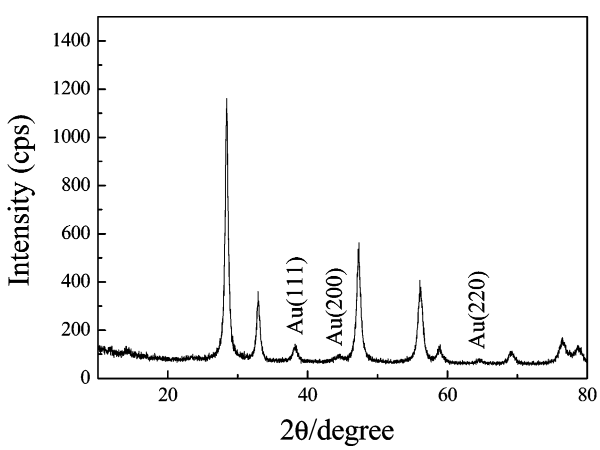

Figure 6. XRD pattern of Au/CeO$_2$ nanorods.

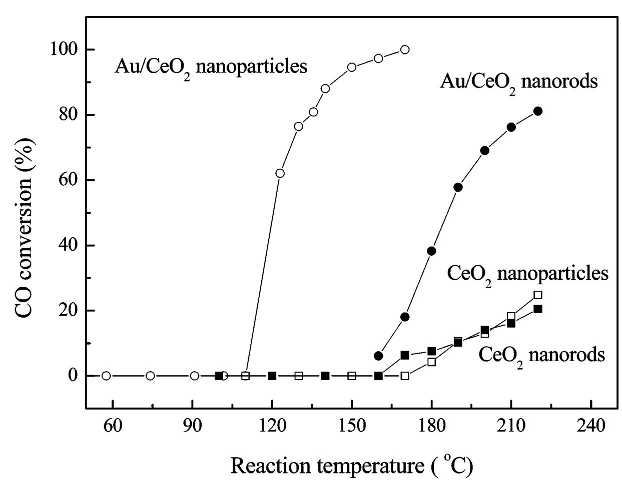

Figure 7. Catalytic activities of CeO$_2$ nanorods and Au/CeO$_2$ nanorods (solid) as compared with CeO$_2$ nanoparticles and Au/CeO$_2$ nanoparticles (open) at different reaction temperatures.

Catalytic activities of CeO$_2$ nanorods and gold nanoparticles on the CeO$_2$ nanorods as a function of reaction temperature are shown in Figure 7. It is noted that the CO conversion increases with increasing reaction temperature for all samples. An 81% CO conversion is achieved at 220 °C for Au/CeO$_2$ nanorods as catalyst, while only 20−22% CO conversion is obtained at the same temperature for pure CeO$_2$ nanorods and nanoparticles as catalyst. The catalytic activity of Au/CeO$_2$ nanorods and Au/CeO$_2$ nanoparticles is much higher than that of pure CeO$_2$ nanorods and nanoparticles. There could be a synergistic interaction between gold and CeO$_2$ nanorods, which is responsible for the high activity. It should be noted that the catalytic activity of Au/CeO$_2$ nanoparticles is measured to be superior in all samples. Recently, Venezia found that the reactive oxygen on the surface of nanocrystalline CeO$_2$ and the strong interaction between cationic gold and ceria may determine the high activity for CO conversion.[32,39] The smaller CeO$_2$ nanoparticles may supply more active sites and contribute to the strong interaction between gold and nanocrystalline CeO$_2$. Therefore, the catalytic activity of Au/CeO$_2$ nanoparticles is better as compared to that of Au/CeO$_2$ nanorods. However, the thermal stability of the Au/

CeO_2 catalyst is also an important factor for application. The CeO_2 nanorods, with the higher crystallinity and larger particle size, have high thermal stability,[1] which enhances the durability of the catalyst.

IV. Conclusion

In summary, uniform single-crystal CeO_2 nanorods have been synthesized through a hydrothermal synthesis in KOH solution at 180 °C for 45 h, without any templates and surfactants. The nanorod formation involves the dehydration of $CeO_2 \cdot 1.1H_2O$ nanoparticles, while the orientation grows along the $\langle 110 \rangle$ direction in KOH solution. The hydrothermal synthesis in alkaline solution is an efficient method for producing large-scale metallic oxide nanorods and can be engineered to produce functional nanostructures under moderate conditions. Subsequently, Au nanoparticles supported on the surface of CeO_2 nanorods were prepared by reducing $HAuCl_4$ impregnated on the nanorods with $NaBH_4$ solution as CO oxidation catalyst, which exhibits a much higher catalytic activity than the pure CeO_2 nanorods.

Acknowledgment. This work is supported by the NCET (Grant 040219), the NSFC (Grants 90206043 and 20271028), and the TNSF (Grants 033804411 and 033602511), China. Financial support from the Australian Research Council (ARC) is also gratefully acknowledged, and H.Y.Z. is indebted to ARC for the QE II fellowship.

References and Notes

(1) Patzke, G. R.; Krumeich, F.; Nesper, R. *Angew. Chem., Int. Ed.* **2002**, *41*, 2446.
(2) Huang, M. H.; Mao, S.; Feick, H.; Yan, H. Q.; Qu, Y. Y.; Kind, H.; Weber, E.; Russo, R.; Yang, P. D. *Science* **2001**, *292*, 1897.
(3) Gao, X. P.; Zheng, Z. F.; Zhu, H. Y.; Pan, G. L.; Bao, J. L.; Wu, F.; Song, D. Y. *Chem. Commun*. **2004**, 1428.
(4) Zhu, H. Y.; Riches, J. D.; Barry, J. C. *Chem. Mater*. **2002**, *14*, 2086.
(5) Zhu, H. Y.; Gao, X. P.; Song, D. Y.; Bai, Y. Q.; Ringer, S. P.; Gao, Z.; Xi, Y. X.; Martens, W.; Riches, J. D.; Frost, R. L. *J. Phys. Chem. B* **2004**, *108*, 4245.
(6) Yang, P. D.; Lieber, C. M. *Science* **1996**, *273*, 1836.
(7) Wang, W. Z.; Zhan, Y. J.; Wang, G. H. *Chem. Commun*. **2001**, 727.
(8) Gao, X. P.; Bao, J. L.; Pan, G. L.; Zhu, H. Y.; Huang, P. X.; Wu, F.; Song, D. Y. *J. Phys. Chem. B* **2004**, *18*, 5547.
(9) Pan, Z. W.; Dai, Z. R.; Wang, Z. L. *Science* **2001**, *291*, 1947.
(10) Lakshmi, B. B.; Patrissi, C. J.; Martin, C. R. *Chem. Mater*. **1997**, *9*, 2544.
(11) Xu, R.; Zeng, H. C. *J. Phys. Chem. B* **2003**, *107*, 12643.
(12) Livage, J. *Chem. Mater*. **1991**, *3*, 578.
(13) Pol, V. G.; Palchik, O.; Gedanken, A.; Felner, I. *J. Phys. Chem. B* **2002**, *106*, 9737.
(14) Kasuga, T.; Hiramatsu, M.; Hoson, A.; Sekino, T.; Niihara, K. *Langmuir* **1998**, *14*, 3160.
(15) Yuan, Z. Y.; Colomer, J. F.; Su, B. L. *Chem. Phys. Lett*. **2002**, *363*, 362.
(16) Gao, X. P.; Zhu, H. Y.; Pan, G. L.; Ye, S. H.; Lan, Y.; Wu, F.; Song, D. Y. *J. Phys. Chem. B* **2004**, *108*, 2868.
(17) Zhu, H. Y.; Lan, Y.; Gao, X. P.; Ringer, S. P.; Zheng, Z. F.; Song, D. Y.; Zhao, J. C. *J. Am. Chem. Soc*. **2005**, *127*, 6730.
(18) Wang, X.; Li, Y. D. *Angew. Chem., Int. Ed*. **2002**, *41*, 4790.
(19) Kosynkin, V. D.; Arzgatkina, A. A.; Ivanov, E. N.; Chtoutsa, M. G.; Grabko, A. I.; Kardapolov, A. V.; Sysina, N. A. *J. Alloys Compd*. **2000**, *303*, 421.
(20) Kleinlogel, C.; Gauckler, L. J. *Adv. Mater*. **2001**, *13*, 1081.
(21) Kaspar, J.; Fornasiero, P.; Graziani, M. *Catal. Today* **1999**, *50*, 285.
(22) Mukherjee, A.; Harrison, D.; Podlaha, E. J. *Electrochem. Solid-State Lett*. **2001**, *4*, D5.
(23) La, R. J.; Hu, Z. A.; Li, H. L.; Shang, X. L.; Yang, Y. Y. *Mater. Sci. Eng., A* **2004**, *367*, 145.
(24) Wu, G. S.; Xie, T.; Yuan, X. Y.; Cheng, B. C.; Zhang, L. D. *Mater. Res. Bull*. **2004**, *39*, 1023.
(25) Sun, C. W.; Li, H.; Wang, Z. X.; Chen, L. Q.; Huang, X. J. *Chem. Lett*. **2004**, *33*, 662.
(26) Vantomme, A.; Yuan, Z. Y.; Du, G. H.; Su, B. L. *Langmuir* **2005**, *21*, 1132.
(27) Yang, R.; Guo, L. *J. Mater. Sci*. **2005**, *40*, 1305.
(28) Carrettin, S.; Concepcion, P.; Corma, A.; Nieto, J. M. L.; Puntes, V. F. *Angew. Chem., Int. Ed.* **2004**, *43*, 2538.
(29) Guzman, J.; Gates, B. C. *J. Am. Chem. Soc*. **2004**, *126*, 2672.
(30) Lee, S.; Fan, C. Y.; Wu, T. P.; Anderson, S. L. *J. Am. Chem. Soc*. **2004**, *126*, 5682.
(31) Guzman, J.; Corma, A. *Chem Commun*. **2005**, 743.
(32) Guzman, J.; Carrettin, S.; Corma, A. *J. Am. Chem. Soc*. **2005**, *127*, 3286.
(33) Salvi, A. M.; Decker, F.; Varsano, F.; Speranza, G. *Surf. Interface Anal.* **2001**, *31*, 255.
(34) Wang, Z. L.; Feng, X. D. *J. Phys. Chem. B* **2003**, *107*, 13563.
(35) Kabalnov, A. *J. Dispersion Sci. Technol*. **2001**, *22*, 1.
(36) Ma, R. Z.; Sasaki, T.; Bando, Y. *J. Am. Chem. Soc*. **2004**, *126*, 10382.
(37) Huang, J. G.; Kunitake, T.; Onoue, S. Y. *Chem. Commun*. **2004**, 1008.
(38) Sudhakar, C.; Vannice, M. A. *Appl. Catal*. **1985**, *14*, 47.
(39) Venezia, A. M.; Pantaleo, G.; Longo, A.; Di Carlo, G.; Casaletto, M. P.; Liotta, F. L.; Deganello, G. *J. Phys. Chem. B* **2005**, *109*, 2821.